Evidence of Redox Relaxation during Thermal Treatment of Soda Lime Silica Glasses Doped with Chromium and Manganese

L. Kido, M. Müller, and C. Rüssel*

Otto-Schott-Institut, Universität Jena, D-07743 Jena, Germany

Received December 8, 2004

A soda lime silica glass with the basic composition $74SiO_2 \cdot 16Na_2O \cdot 10CaO$ doped with MnO and Cr_2O_3 was studied by high-temperature UV−vis−NIR spectroscopy. The measurements were carried out at temperatures in the range from 25 to 800 °C. The spectra were deconvoluted especially with respect to the absorption peaks caused by Cr^{6+} and Mn^{3+}. Up to a temperature of around 520 °C, the absorptivities of peaks due to Cr^{6+} and Mn^{3+} decreased with temperature in the same way as in glasses doped with only one of these polyvalent elements. At higher temperature, the absorptivity of peaks caused by Cr^{6+} increases while those attributed to Mn^{3+} decreases. This is due to the redox reaction $Cr^{6+} + 3Mn^{2+} \rightleftarrows Cr^{3+} + 3Mn^{3+}$, which is shifted to the left with increasing temperature. At temperatures < 520 °C, the redox reaction is frozen in. If the glass is heated more slowly, the intensity of the Cr^{6+} peaks decreases at temperatures > 520 °C and re-increases at temperatures > 600 °C. If a temperature in the range from 530 to 590 °C is kept, the intensity of the Cr^{6+} decreases steadily according to an exponential law. From this dependency, redox relaxation times were calculated. Thermodynamics and kinetics of the redox reaction are illustrated by numerical calculations. This is the first experimental evidence for redox relaxation in glasses.

1. Introduction

Most transition metal ions may occur in glass and the melts they are prepared from in different oxidation states, i.e., they are polyvalent.[1−9] Different oxidation states, however, also result in different absorptivities of light, especially in the wavelength range from 300 to 3000 nm.[10,11] At high temperatures, the redox ratio of transition-metal ions and also that of polyvalent main group elements can readily be described by the total concentrations and the activity of physically dissolved oxygen.[8−11]

$$A^{(n-z)+} + z/4O_2 \overset{K'_A}{\rightleftarrows} A^{n+} + z/2O^{2-} \quad (1)$$

The equilibrium constant K'_A can be defined as

$$K'_A(T) = \frac{a_{A^{n+}} a_{O^{2-}}{}^{z/2}}{a_{A^{(n-z)+}} a_{O_2}{}^{z/4}} \quad (2)$$

where a_i are the activities of the respective species. Although the species O^{2-} scarcely occurs in the melt, it effectively remains constant because it is in equilibrium with the concentration of nonbridging oxygen. Furthermore for small concentrations of the species A (usually <1 mol %), the redox ratio does not depend on [A], and hence if referenced to ideally diluted solutions, the activity coefficients can be considered as unity and the activities be replaced by the respective concentrations. Nevertheless the equilibrium constant depends on the melt composition (see, e.g., ref 9).

$$K_A(T) = \frac{[A^{n+}]}{[A^{(n-z)+}] a_{O_2}{}^{z/4}} \quad (3)$$

Redox equilibrium constants depend strongly on the temperature and get larger with decreasing temperature. Nevertheless, the diffusivity of the oxygen in highly viscous silicates is too slow to affect the redox ratios when a melt is cooled in conventional laboratory experiments (some 10−100 g melt in a crucible and cooling rates of $1-100\ K \cdot min^{-1}$, concentrations [A] > 0.1 mol %). Therefore, the redox ratio remains constant during cooling, if only one type of polyvalent element is present, due to the lack of a reaction partner.[12,13]

This situation changes, if more than one type of polyvalent element is present. Here at high temperature, each of the redox couples is in equilibrium with the physically dissolved oxygen and hence the redox ratio of each of them is the same as in a melt solely doped with the respective polyvalent element (if a_{O_2} is the same). However, during cooling, the following redox reaction may take place.[14−18]

(1) Paul, A. *J. Non-Cryst. Solids* **1985**, *71*, 269.
(2) Paul, A.; Douglas, Z. W. *Phys. Chem. Glasses* **1965**, *6*, 207.
(3) Hirashima, H.; Yoshida, T.; Brückner, R. *Glastech. Ber.* **1988**, *61*, 283.
(4) Lauer, H. V. *Phys. Chem. Glasses* **1977**, *18*, 49.
(5) Freude, E.; Rüssel, C. *Glastech. Ber.* **1987**, *60*, 202.
(6) Schreiber, H. D.; Hockman, A. L. *J. Am. Ceram. Soc.* **1987**, *70*, 591.
(7) Schreiber, H. D.; Kozak, S. J.; Merkel, R. C.; Balazs, G. B.; Jones, P. W. *J. Non-Cryst. Solids* **1986**, *84*, 186.
(8) Xiang, Z. D.; Cable, M. *Phys. Chem. Glasses* **1997**, *38*, 167.
(9) Rüssel, C.; Wiedenroth, A. *Chem. Geol.* **2004**, *213*, 125.
(10) Paul, A. *Chemistry of Glasses*; Chapman & Hall: New York, 1982.
(11) Weyl, W. A. *Colored Glasses*; Soc. Glass Technol.: Sheffield, 1967.
(12) Kohl, R.; Schaeffer, H. A. *Diff. Defect Data* **1987**, *53 & 54*, 325.
(13) Rüssel, C.; Kohl, R.; Schaeffer, H. A. *Glastech. Ber.* **1988**, *61*, 209.

10.1021/cm040202k CCC: $30.25
Published on Web 06/25/2005

$$z\cdot B^{(m-y)+} + y\cdot A^{n+} \rightleftarrows z\cdot B^{m+} + y\cdot A^{(n-z)+} \quad (4)$$

While the diffusion of oxygen in the melt requires diffusion paths in the millimeter to centimeter range, the homogeneous redox reaction according to eq 4 requires diffusion paths in the nanometer range. In the past, it has been shown that this type of redox reaction may strongly affect the redox ratios in cooled glasses. This has been shown in equilibration experiments when melts solely doped with one polyvalent element and melts doped with two types of polyvalent elements were studied. Then, in many cases the redox ratios were not the same after cooling (see, e.g., ref 8). By means of high-temperature electron paramagnetic resonance[17] and high-temperature UV−vis−NIR spectroscopy,[14,15,18] redox reactions have been studied in situ. Here, it has shown that, below a certain temperature (usually around T_g), the redox reaction is frozen in. At higher temperatures, the redox ratios are notably shifted with temperature. Up to now, glasses containing iron and arsenic,[14,17] glasses doped with copper and antimony or tin,[15] as well as glasses doped with chromium and manganese[18] have been studied. In the latter system, the Cr^{6+} concentration increases with temperature while the Mn^{3+} concentration decreases.[18] Under the experimental conditions supplied, the redox reaction was frozen in at temperatures < 600 °C. The shift in the redox ratios was quantitatively explained in ref 18 by thermodynamic data ($\Delta H^\circ_{Cr^{3+}/Cr^{6+}} = 76 kJ\cdot mol^{-1}$, $\Delta S^\circ_{Cr^{3+}/Cr^{6+}} = 54\ J\cdot mol^{-1}\ K^{-1}$) determined voltammetrically at temperatures in the range from 800 to 1300 °C. $\Delta G^\circ_{Mn^{2+}/Mn^{3+}} = -103.6\ kJ\cdot mol^{-1}$, was determined by equilibrating a melt only containing manganese with air and subsequent quenching. Additionally, $\Delta S^\circ_{Mn^{2+}/Mn^{3+}}$ (=121.8 $J\cdot mol^{-1}\ K^{-1}$) was fitted to the data from equilibrated samples containing both chromium and manganese.[18] From these data, the equilibrium constants K of the redox reaction $Cr^{6+} + 3Mn^{2+} \rightleftarrows Cr^{3+} + 3Mn^{3+}$ can be calculated: 10.6 and 0.36 for 1400 and 600 °C, respectively. This paper provides a study of the kinetics of this redox reaction using high-temperature UV−vis−NIR spectroscopy. For that purpose, heating rates were varied and the temperatures were kept at certain values in order to study the redox relaxation kinetics.

2. Theory

Both manganese and chromium form redox equilibria with the physically dissolved oxygen of the melt at high temperatures. The respective equilibrium constants $K_A(T)$ and $K_B(T)$ depend on temperature.

$$-RT \ln K_A(T) = \Delta G^\circ_A = \Delta H^\circ_A - T\Delta S^\circ_A \quad (5)$$

$$-RT \ln K_B(T) = \Delta G^\circ_B = \Delta H^\circ_B - T\Delta S^\circ_B \quad (6)$$

where ΔG°, ΔH°, and ΔS° are the standard free enthalpy, the standard enthalpy, and the standard entropy of the redox reaction, respectively. In the case of manganese and chromium doped melts, the following reaction may take place

$$Cr^{3+} + 3Mn^{3+} \overset{K_{Cr/Mn}(T)}{\rightleftharpoons} Cr^{6+} + 3Mn^{2+} \quad (7)$$

The equilibrium constant $K_{Cr/Mn}(T)$ is given by eqs 5 and 6.[14] Since $\Delta H^\circ_{Cr} \neq 3\Delta H^\circ_{Mn}$, the equilibrium depends on

$$K_{Cr/Mn}(T) = \frac{K_{Mn}{}^3}{K_{Cr}} = \exp[(\Delta H^\circ_{Cr} - 3\Delta H^\circ_{Mn})/(RT)] \exp[(\Delta S^\circ_{Cr} - 3\Delta S^\circ_{Mn})/R] \quad (8)$$

temperature. The kinetics of the reaction according to eq 7 is given by where k_+ and k_- are the rate constants of the

$$\frac{dx}{dt} = ([Mn^{3+}]_0 + x)^3([Cr^{3+}]_0 + x/3)k_+ - ([Mn^{2+}]_0 - x)^3([Cr^{6+}]_0 - x/3)k_- \quad (9)$$

forward and backward reactions, respectively. $[A]_0$ is the initial concentration of the respective species (at $t = 0$). The quotient of k_+ and k_- is equal to the equilibrium constant

$$\frac{k_+}{k_-} = K_{Cr/Mn}(T) \quad (10)$$

Both k_+ and k_- depend on temperature according to Arrhenius equation.

$$k_+ = k \exp\left(-\frac{E_+}{RT}\right) \quad (11)$$

$$k_- = k \exp\left(\frac{\Delta S^\circ_{Cr/Mn}}{R}\right) \exp\left(-\frac{E_+ + \Delta H^\circ_{Cr/Mn}}{RT}\right) \quad (12)$$

For small deviations from an equilibrium, ΔC_0, the system will relax according to

$$\Delta C = \Delta C_0 \exp(-t/\tau) \quad (13)$$

where τ is the relaxation time which depends on the rate constant and for reaction orders > 1 on the concentrations of the reacting species. For the reaction according to eq 7, τ is given by

$$\tau = \left\{k_+\left(\frac{1}{3}[Mn^{3+}] + 3[Cr^{3+}]\right)[Mn^{3+}]^2 + k_-\left(\frac{1}{3}[Mn^{2+}] + 3[Cr^{6+}]\right)[Mn^{2+}]^2\right\}^{-1} \quad (14)$$

In glass science, two relaxation processes are well-known: mechanical and electrical relaxation. Mechanical relaxation is mainly observed at temperatures around the glass transition temperature, T_g, and controls, e.g., stress relaxation and the increase in density during tempering of rapidly cooled glass samples. The simplest description is Maxwell's kinetics of relaxation assuming Newtonian flow behavior. The attributed relaxation time τ is directly proportional to the viscosity η.[19]

(14) Schirmer, H.; Müller, Ma.; Rüssel, C. *Glass Sci. Technol*. **2002**, *76*, 49.
(15) Kido, L.; Müller, Ma.; Rüssel, C. *Phys. Chem. Glasses* **2004**, *45*, 21.
(16) Rüssel, C. *Glastech. Ber*. **1989**, *62*, 199.
(17) Gravanis, G.; Rüssel, C. *Glastech. Ber*. **1989**, *62*, 345.
(18) Kido, L.; Müller, Ma.; Rüssel, C. *J. Non-Cryst. Solids*. In press.
(19) Gutzow, I.; Schmelzer, J. *The Vitreous State*; Springer: Berlin, Heidelberg, New York, 1995.

$$\tau = \frac{\eta}{q} \tag{15}$$

with q = shear modulus (typical: 2×10^{11} Pa). At the glass transition temperature ($\eta = 10^{13}$ dPas), τ is approximately 50 s.[20] More complex concepts assume more than one,[21] or even a distribution of relaxation times, include non-Newtonian flow[22] or, however, take into account the dependency of the viscosity on the cooling rate. The latter is described by the Bartenev equation.[23]

$$q = A \exp\frac{E_q}{RT_g} \tag{16}$$

where q = cooling rate and A is a constant depending on the glass composition. The energy E_q is approximately equal to the activation energy of the viscous flow (assuming Arrhenius behavior at T_g). The effect of temperature history can be quantified by the fictive temperature of viscous flow. The fictive temperature was first introduced by Tool.[24] It is equal to that temperature the structure or a certain property is attributed to an equilibrium state.

3. Experimental Procedure

Glasses with the basic composition $16Na_2O{\cdot}10CaO{\cdot}74SiO_2$ doped with MnO and Cr_2O_3 were melted from reagent grades Na_2CO_3, $CaCO_3$, SiO_2, $MnCO_3$, and Cr_2O_3 in a platinum crucible at 1480 °C. The glasses were cast on a graphite mould preheated to 530 °C and then cooled to room temperature supplying a cooling rate of 30 K·h^{-1}. Cylindrical samples with a diameter of 6 mm and a thickness of 0.2 mm were prepared and polished to optical quality.

UV−vis−NIR transmission spectra were recorded with a specially constructed experimental arrangement in the temperature range from 25 to 800 °C. The arrangement consisted of a microscope heating stage (TS 1500, LINCAM, Waterfield, Great Britain) inside which the samples were located. The light from a Xe lamp was conducted by a SiO_2 light guide into the heating stage. The transmitted light was conducted by an SiO_2 light guide into a diode array spectrometer (InstaSpec IIa, L.O.T.).

The spectra recorded exhibited broad absorption bands caused by Cr^{3+} (15 200 and 22 600 cm^{-1}), Cr^{6+} (27 500 cm^{-1}), and Mn^{3+} (20 300 and a shoulder at 15 100 cm^{-1}). Each recorded spectrum was carefully deconvoluted into the respective Gaussian absorption bands. Because of the strong overlap of the bands at around 15 000 cm^{-1} caused by both Mn^{3+} and Cr^{3+}, the lines of Cr^{6+} at 27 500 cm^{-1} and of Mn^{3+} at 20 300 cm^{-1} were used for a further description of redox equilibria and reactions.

The glass transition temperature was measured by dilatometry (Netzsch 402 E); the viscosities were determined by beam bending viscometry (Bähr VIS 403) in the temperature range from 570 to 622 °C.

4. Results

Figure 1 presents absorption spectra recorded in a glass doped with 0.67 MnO and 0.11 Cr_2O_3 as a function of the temperature during heating, supplying a heating rate of 20 K·min^{-1}. In the room-temperature spectrum, distinct lines at around 20 300 and 27 500 cm^{-1} as well as a broad shoulder at 15 100 cm^{-1} is observed. The intensity of the line at around 27 500 cm^{-1} is smaller at 400 °C, however, is notably larger at 700 and 800 °C. The absorptions at around 20 300 cm^{-1} steadily decrease with increasing temperature. It should be noted that the UV cut off is shifted to the visible range with increasing temperature.

Parts a and b of Figure 2 show the attributed absorptivities of the lines at 27 500 cm^{-1} due to Cr^{6+} and at 20 300 caused by Mn^{3+}, obtained after deconvolution. Up to a temperature

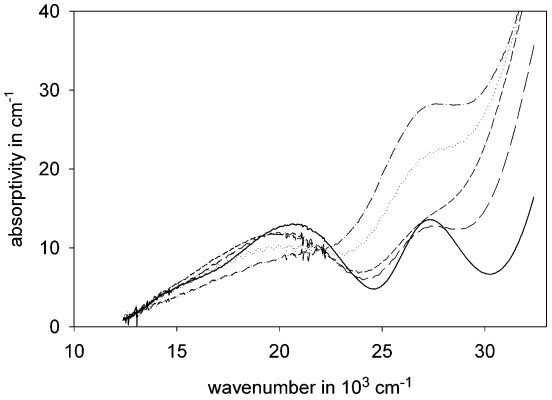

Figure 1. Absorption spectra of a glass doped with 0.67 mol % MnO and 0.11 mol % Cr_2O_3, recorded at various temperatures: solid line, 25 °C; long-dashed line, 400 °C; short-dashed line, 600 °C; dotted line, 700 °C; dot-dashed line, 800 °C.

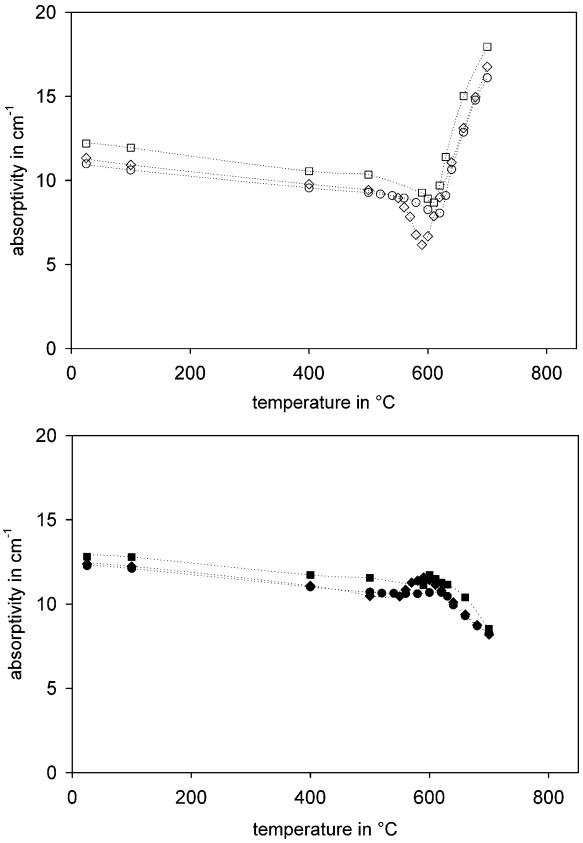

Figure 2. (a) 27 500 cm^{-1} (Cr^{6+}, hollow symbols) and (b) absorption maxima of the peaks at 20 300 cm^{-1} (Mn^{3+}, solid symbols) measured in a glass doped with 0.67 mol % MnO and 0.11 mol % Cr_2O_3 during heating (◇) 1 K·min^{-1}, (□) 5 K·min^{-1}, and (○) 20 K·min^{-1}.

(20) Scholze, H. *Glas−Natur, Struktur und Eigenschaften*; Springer: Berlin, Heidelberg, New York, 1995; p 43.
(21) van Zee, A. F.; Noritake, H. M. *J. Am. Ceram. Soc.* **1958**, *41*, 164.
(22) DeBast, J.; Gilard, P. *Phys. Chem. Glasses* **1963**, *4*, 117.
(23) Bartenev, G. M. *Akademii Nauk S.S.S.R.* **1951**, *76*, 227.
(24) Tool, A. Q. *J. Am. Ceram. Soc.* **1946**, *29*, 240.

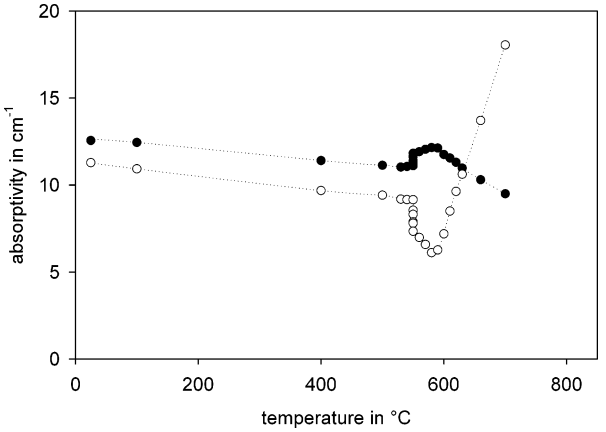

Figure 3. Absorption maxima of the peaks at 20 300 cm^{-1} (Mn^{3+}) and 27 500 cm^{-1} (Cr^{6+}) measured in a glass doped with 0.67 mol % MnO and 0.11 mol % Cr_2O_3. The glass was heated to 550 °C with a heating rate of 20 K·min^{-1}, kept for 1 h at this temperature, and then further heated with 1 K·min^{-1}.

of 600 °C, both the Mn^{3+} as well as the Cr^{6+} absorptivities decrease steadily. It should be noted that approximately the same decrease is also observed in glasses doped with only one of these polyvalent elements (see ref 18). At temperatures larger than 600 °C, the Cr^{6+} absorptivities strongly increase while those of Mn^{3+} decrease with increasing temperature. It should be noted that in glasses doped with only one polyvalent element, i.e., either with Cr_2O_3 or MnO, the absorptivities steadily decrease also in the temperature range from 600 to 800 °C. Parts a and b of Figure 2 also show absorptivities obtained from the same glass composition, however, the spectra were recorded using heating rates of 1 and 5 K·min^{-1}. The absorptivities up to a temperature of 530 °C are approximately the same and do not significantly depend on the heating rate. In analogy, also the absorptivities above 650 °C are not affected by the heating rate. However, in the range from 530 to 650 °C, the absorptivities depend on heating rates. At a heating rate of 20 K·min^{-1}, the absorptivities of Cr^{6+} gets only slightly smaller than those extrapolated from the temperature dependence in the range from 25 to 500 °C. The minimum occurs at a temperature of 620 °C. The re-increase in absorptivity is observed above 625 °C. At a heating rate of 5 K·min^{-1}, the minimum is observed at 610 °C and is attributed to smaller absorptivities. At a heating rate of 1 K·min^{-1}, the absorptivity decreases strongly at temperatures above 550 °C, reaches the minimum at 600 °C, and then increases again. In the temperature range from 530 to 650 °C at all three heating rates the absorptivities of Mn^{3+} show the opposite behavior. When the Cr^{6+} absorptivity increases, the Mn^{3+} absorption decreases and vice versa.

In Figure 3, results from a somewhat different experiment are shown. The sample was heated with a rate of 20 K·min^{-1} up to a temperature of 550 °C and then kept for 1 h. Subsequently, the sample was further heated with a rate of 1 K·min^{-1}. The absorptivities below 550 and above 595 °C are the same as those shown in Figure 2 for a heating rate of 1 K·min^{-1}. While the sample was kept at 550 °C, the absorptivities of Cr^{6+} decrease continuously with time from 9.4 to 7.25 cm^{-1}. In Figure 4, the decrease in the Cr^{6+} and the increase in the Mn^{3+} absorptivity while keeping the

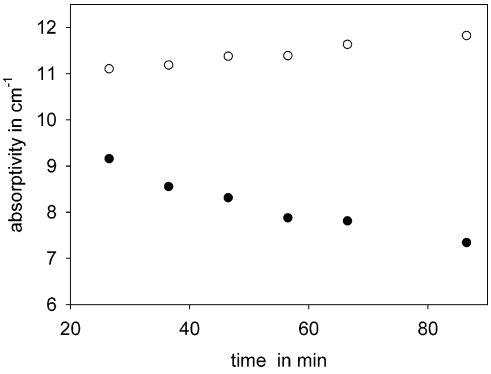

Figure 4. Absorption maxima of the peaks at 20 300 cm^{-1} (Mn^{3+}, hollow symbols) and 27 500 cm^{-1} (Cr^{6+}, solid symbols) measured in a glass doped with 0.67 mol % MnO and 0.11 mol % Cr_2O_3 as a function of time during thermal treatment at 550 °C.

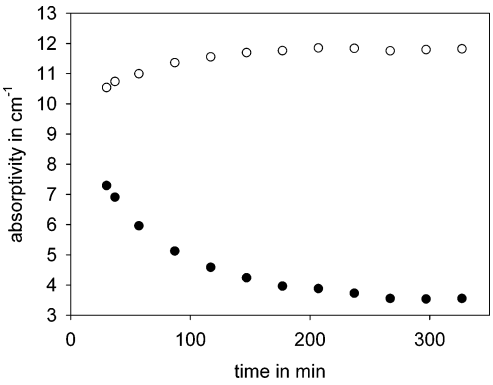

Figure 5. Absorption maxima of the peaks at 20 300 cm^{-1} (Mn^{3+}, hollow symbols) and 27 500 cm^{-1} (Cr^{6+}, solid symbols) measured in a glass doped with 0.67 mol % MnO and 0.11 mol % Cr_2O_3 as a function of time during thermal treatment at 560 °C.

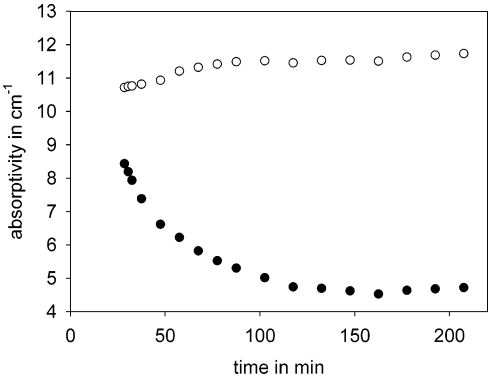

Figure 6. Absorption maxima of the peaks at 20 300 cm^{-1} (Mn^{3+}, hollow symbols) and 27 500 cm^{-1} (Cr^{6+}, solid symbols) measured in a glass doped with 0.67 mol % MnO and 0.11 mol % Cr_2O_3 as a function of time during thermal treatment at 570 °C.

sample at 550 °C is shown as a function of time. In Figures 5 and 6, absorptivities of Cr^{6+} and Mn^{3+} are shown as a function of the time. Here the samples were heated with a rate of 20 K·min^{-1} and then kept at 560 and 570 °C for 5 and 3 h, respectively. At both temperatures, the Cr^{6+} absorption decreases and the Mn^{3+} absorption increases with time. At temperatures of 560 and 570 °C, constant absorptivities are reached after keeping the samples for around 4 and 2 h, respectively.

The glass transition temperature measured by dilatometry was 552 ± 2 °C, the viscosities at 573 and 622.6 °C were 1.68×10^{12} and 1.33×10^{10} dPas, respectively.

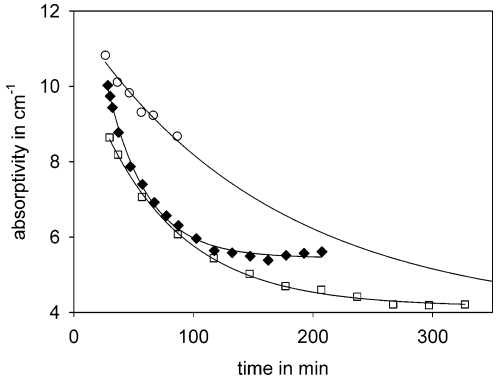

Figure 7. Absorption of Cr^{6+} as a function of time for (○) 550 °C, (□) 560 °C, and (◆) 570 °C.

5. Discussion

In the system studied, the redox equilibrium is shifted during changing the temperature. At temperatures > 650 °C, the redox ratio does not depend on the heating rate. So the redox reaction can be considered to be in equilibrium within the time scale of the measurements performed. At temperatures < 520 °C, the absorptivities do not depend on the heating rate and are constant at a given temperature. Here, the redox ratio does not change and the equilibrium is frozen. The same behavior has already been reported for the Mn/Cr system studied in this paper and also from other systems, such as Fe/As[14] or Cu/Sb.[15]

As shown in Figures 4−6, the absorptivities and hence the redox ratios Mn^{3+}/Mn^{2+} and Cr^{6+}/Cr^{3+} change with time at temperatures in the range from 550 to 570 °C. In Figure 7, the Cr^{6+} absorptions are shown. At 560 and 570 °C, within the limits of error, constant values are obtained after 4 and 2 h, respectively. The solid lines drawn were fitted to an exponential decay, i.e., to $y = a + b\exp(-t/\tau)$, where a and b are constants. The fit parameter τ has the physical meaning of a relaxation time. At a temperature of 550 °C, a limiting value, attributed to the redox equilibrium, is not reached within the time scale of the measurement. However, from the thermodynamic data given above and the extinction coefficient of Cr^{6+} (56 000 cm^{-1}·mol %$^{-1}$),[18] the absorptivities at equilibrium conditions can be calculated ($a_{Cr^{6+}} = 5.07$ cm^{-1}). By assumption that this value can be reached at infinitely large times, an exponential decay can also be fitted in this case (see also solid line in Figure 7). The relaxation times obtained were 9460, 4150, and 2000 s (error ± 5%) for 550, 560, and 570 °C, respectively.

From relaxation times and the respective equilibrium concentrations of the redox species, the rate constants k_+ and k_- can be calculated using eq 14. The respective concentrations, as well as the equilibrium constant $K_{Mn/Cr}$, were calculated from the thermodynamics. This results in k_+ values of 0.7×10^{-2}, 1.86×10^{-2}, and 4.47×10^{-2} s^{-1}·mol %$^{-3}$ (error ± 5%) for 550, 560, and 570 °C, respectively. Figure 8 shows an Arrhenius plot of the rate constant k_+. A linear correlation is observed from which an activation energy of 535 ± 29 kJ·mol^{-1} and a pre-exponential factor of 62.3×10^{30} s^{-1}·mol %$^{-3}$ is obtained. The rate constant and equilibrium constant and their temperature dependencies enable to solve eq 9 numerically.

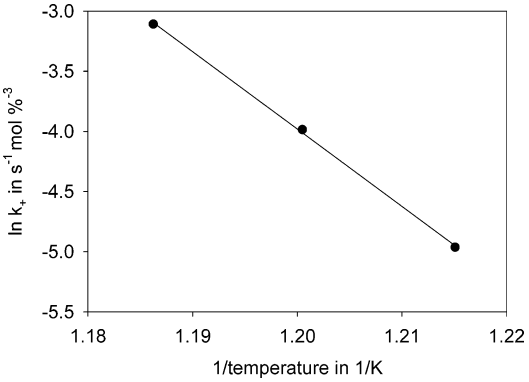

Figure 8. Arrhenius plot of the rate constant k_+.

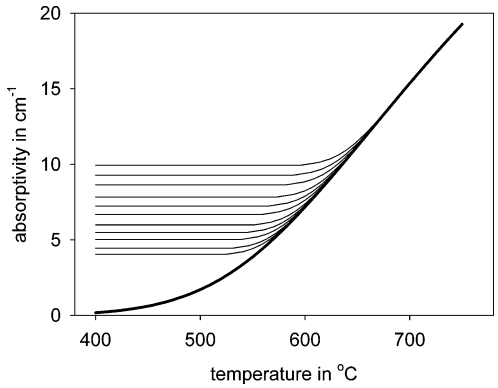

Figure 9. Theoretically calculated Cr^{6+} absorptivities (normalized to room temperature for different cooling rates). From the top: 2000, 1000, 500, 200, 100, 50, 20, 10, 5, 2, and 1 K·min^{-1}. The thick line indicates equilibrium values.

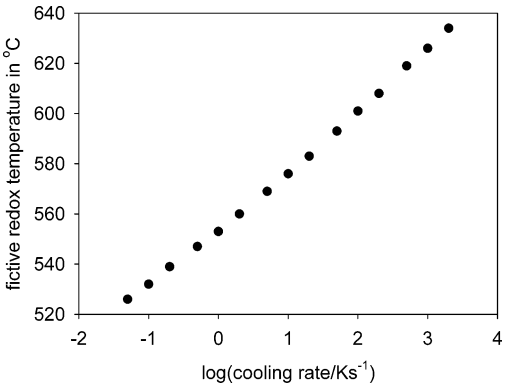

Figure 10. Calculated fictive redox temperatures as a function of the cooling rate.

Figure 9 shows results from numerical calculations for the cooling of the melt. The thick line is attributed to the equilibrium, while the thin lines were obtained for different cooling rates which were in the range from 1 to 2000 K·min^{-1}. At all these cooling rates, the system is in equilibrium at temperatures > 650 °C and the redox reaction is frozen below 520 °C. The redox ratio of the cooled glass is attributed to the equilibrium value at 634 °C. In analogy to mechanic relaxation (see eq 15), these temperatures, in the following, are denoted as fictive redox temperatures. The smaller the cooling rate, the lower the temperature, first deviations from the equilibrium occur, and the lower the fictive redox temperature. The fictive redox temperature is shown in Figure 10. Within the studied cooling rate range (0.05 to 2000 K·min^{-1}), it varies over more than 100 K.

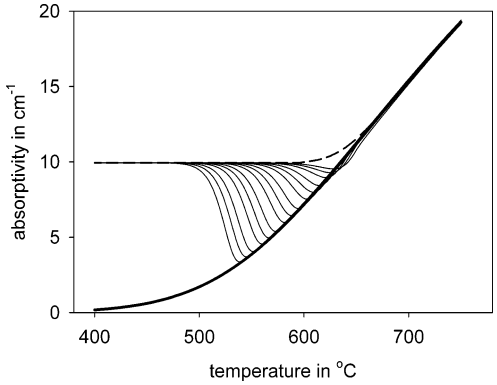

Figure 11. Theoretically calculated Cr^{6+} absorptivities (normalized to room temperature for different heating rates). Solid lines: 2000, 1000, 500, 200, 100, 50, 20, 10, 5, 2, 1, 0.5, 0.2, 0.1, and 0.05 K·min^{-1} (from the top). Dashed line, during cooling; thick line, equilibrium values.

In Figure 11, the behavior during heating of the sample is shown. In analogy to Figure 9, the heating rate was varied in a wide range (0.05 to 2000 K·min^{-1}). At temperatures < 480 °C, the redox ratio is equal to that during cooling and does not change with temperature, while at temperatures > 650 °C, the redox ratio is equal to that of the equilibrium (see thick line). Between, the redox ratio is affected by the heating rate. It first decreases and after reaching the equilibrium value at the respective temperature increases again. The decrease in the absorptivities (corrected to room temperature) is largest at the smallest heating rate supplied. Here, it decreases from initially 10 to 3.5 cm^{-1}, i.e., around the factor 3.

The viscosity data and T_g ($\eta = 10^{13}$ dPas) were fitted to a Vogel−Fulcher−Tammann-type equation ($\eta = 3.951 \times 10^7$ dPas exp(1555 K/(T − 427 K))). From those data, the activation energy of an Arrhenius type equation ($\eta = A$ exp(E_η/RT)) was calculated. This resulted in an activation energy of 562 kJ·mol^{-1} at the glass transition temperature (T_g = 552 °C), which is fairly equivalent to a value of 550 kJ·mol^{-1} given in the literature for a glass with the composition $16Na_2O{\cdot}10CaO{\cdot}74SiO_2$.[20] It should be stated that the activation energy attributed to the viscosity and that attributed to the redox reaction (535 ± 29 kJ·mol^{-1}) are, within the limits of error, in agreement.

In principle, the observed kinetic hindrance of the redox reaction may have two reasons: limited diffusion of the redox species as well as a hindered electron-transfer reaction. Diffusion coefficients of glass melt components differ by up to 6 orders of magnitude, depending on the incorporation of the respective species.[25] Hence, the Stokes−Einstein equation is not valid in glasses and glass-forming melts. This is mainly known from voltammetric measurements typically carried out at temperatures > 1000 °C. Here, monovalent cations, incorporated as network modifiers, possess much larger diffusion coefficients than components, such as Sb^{5+} incorporated as network formers. However, only few data on the diffusivities of polyvalent ions at temperatures around T_g are available in the literature. Besides data on tin diffusivities (activation energy = 63.6 kJ·mol^{-1}),[26] only iron tracer diffusion coefficients are reported. Here, depending on the Fe^{2+}/Fe^{3+} redox ratio, activation energies in the range from 169 to 346 kJ·mol^{-1} are given[27] for a soda lime silica glass composition. These activation energies are much smaller than those of the viscous flow (at T_g) and the redox kinetics described above. It should be noted that also at temperatures >1000 °C, voltammetrically determined diffusion coefficients possess much smaller activation energies than the viscous flow.[25] Hence, it should be concluded that diffusion of the redox species is not the rate determining step for the redox reaction. Polyvalent species usually are incorporated in each redox state in a different manner in a glass. Therefore, redox reactions in glasses should be assumed to run parallel with changes in the respective coordination spheres. Hence, for redox reactions Si−O bonds are broken or formed. Since this is closely related to viscous flow, similar activation energies of redox reactions and viscous flow are not surprising.

Conclusions

While changing the temperature, in soda lime silicate glasses doped with MnO and Cr_2O_3, a redox reaction occurs at temperatures > 520 °C. With increasing temperature, this reaction is shifted toward Cr^{6+} and Mn^{2+}. At temperatures < 520 °C, the reaction is frozen in, while it is in equilibrium at temperatures > 600 °C (both within the time scale of the experiment performed). During thermal treatment of the sample at temperatures in the range from 530 to 600 °C, the absorptions caused by Cr^{6+} decrease with time, while those attributed to Mn^{3+} increase with time. The relaxation times are in the range from 9460 to 2000 s for temperatures of 550 to 570 °C, respectively. This is the first experimental evidence for redox relaxation in glasses.

CM040202K

(25) Rüssel, C. *J. Non-Cryst. Solids* **1991**, *134*, 133.
(26) Sanyal, A. S. *J. Mukerji, Phys. Chem. Glasses* **1983**, *24*, 79.
(27) Köhler, W.; Frischat, G. H. *Phys. Chem. Glasses* **1978**, *19*, 103.